Photolysis of the CH_4 observed in Titan's atmosphere should give a predictable source of H_2; this was estimated by Hunten (*19*) from the photochemical results of Strobel (*36*). It is 9×10^9 cm^{-2} sec^{-1}, referred to a radius of approximately 3000 km. The total escape rate is therefore $E(H_2) = 3.4 \times 10^{27}$ sec^{-1}.

The source of the H actually observed in the torus is probably less than the H_2 source. Strobel (*36*) included an "ionospheric source" of 10^8 H atoms cm^{-2} sec^{-1}, most of which probably would escape. The model predicts an escape rate of 6×10^8 cm^{-2} sec^{-1} from methane photolysis. We should also examine the ionospheric source. At the subsolar point, N_2^+ is presumably being produced at a column rate of 4×10^8 cm^{-2} sec^{-1}. It reacts with H_2 by

$$N_2^+ + H_2 \rightarrow N_2H^+ + H \qquad (1)$$

$$N_2H^+ + e \rightarrow N_2 + H \qquad (2)$$

to produce two H atoms for each N_2^+.

Most of the H atoms will escape thermally. The globally averaged escape rate is $\simeq 1.4 \times 10^{27}$ sec^{-1} for the ionospheric and methane sources (*37*), just the quantity required by the torus. Additional H atoms may be supplied from ionization of H_2 in the torus region followed by

$$H_2^+ + H_2 \rightarrow H_3^+ + H \qquad (3)$$

and subsequent dissociative recombination of H_3^+.

A. L. BROADFOOT, B. R. SANDEL
D. E. SHEMANSKY, J. B. HOLBERG
G. R. SMITH
Earth and Space Sciences Institute, University of Southern California, Tucson, Arizona 85713
D. F. STROBEL
Naval Research Laboratory, Washington, D.C. 20375
J. C. MCCONNELL
York University, Ontario, Canada M3J 1P3
S. KUMAR
University of Southern California, Los Angeles 90007
D. M. HUNTEN
University of Arizona, Tucson 85721
S. K. ATREYA, T. M. DONAHUE
University of Michigan, Ann Arbor 48109
H. W. MOOS
Johns Hopkins University, Baltimore, Maryland 21218
J. L. BERTAUX, J. E. BLAMONT
Service D'Aeronomie du CNRS, Verrieres le Buisson, France
R. B. POMPHREY, S. LINICK
Jet Propulsion Laboratory, Pasadena, California 91103

References and Notes

1. Details of the instrument and data analysis procedure are given by A. L. Broadfoot *et al.*, *J. Geophys. Res.*, in press.
2. H. Weiser, R. C. Vitz, H. W. Moos, *Science* **197**, 755 (1977).
3. J. T. Clarke, H. W. Moos, S. K. Atreya, A. L. Lane, *Nature (London)*, in press.
4. E. S. Barker, S. Cazes, C. Emerich, A. Vidal-Madjar, T. Owen, *Astrophys. J.*, **242**, 383 (1980).
5. J. C. McConnell, B. R. Sandel, A. L. Broadfoot, *Icarus* **43**, 128 (1980).
6. A. L. Broadfoot *et al.*, *Science* **204**, 979 (1979).
7. H. E. Hinteregger, private communication.
8. D. L. Judge, F.-M. Wu, R. W. Carlson, *Science* **207**, 431 (1980).
9. N. F. Ness, M. H. Acuña, R. P. Lepping, J. E. P. Connerney, K. W. Behannon, L. F. Burlaga, F. M. Neubauer, *Science* **212**, 211 (1981).
10. During the north-south map sequence, which covered a complete rotation of the planet, the UVS slit was scanned repeatedly from north pole to south pole as the planet rotated beneath the spacecraft.
11. J. W. Warwick *et al.*, *Science* **212**, 239 (1981).
12. G. L. Tyler, V. R. Eshleman, J. Y. Anderson, G. S. Levy, G. F. Lindal, G. E. Wood, T. A. Croft, *ibid.*, p. 201.
13. L. Froidevaux and A. P. Ingersoll, *J. Geophys. Res.* **85**, 5948 (1980).
14. T. Gehrels, *Science* **207**, 434 (1980).
15. R. W. Carlson, *Nature (London)* **283**, 461 (1980).
16. J. Blamont, in *The Rings of Saturn* (NASA SP-343, Washington, D.C., 1974).
17. M. Dennefeld, *Int. Astron. Union Symp.* **65**, 471 (1974).
18. J. S. Lewis, *Icarus* **15**, 174 (1971).
19. D. M. Hunten, in *Planetary Satellites*, J. A. Burns, Ed. (Univ. of Arizona Press, Tucson, 1977).
20. S. K. Atreya, T. M. Donahue, W. R. Kuhn, *Science* **201**, 611 (1978).
21. R. Hanel *et al.*, *ibid.* **212**, 193 (1981).
22. F. Fischer, G. Stasek, G. Schmidtke, *Geophys. Res. Lett.* **11**, 1003 (1980).
23. E. C. Zipf and R. W. McLaughlin, *Planet. Space Sci.* **26**, 449 (1978).
24. E. C. Zipf, private communication.
25. J. F. M. Aarts and F. J. DeHeer, *Physica* **52**, 45 (1971).
26. M. J. Mumma and E. C. Zipf, *J. Chem. Phys.* **55**, 5582 (1971).
27. E. J. Stone and E. C. Zipf, *ibid.* **58**, 4278 (1973).
28. H. F. Winters, *ibid.* **44**, 1472 (1966).
29. E. S. Oran, P. S. Julienne, D. F. Strobel, *J. Geophys. Res.* **80**, 3068 (1975).
30. D. F. Strobel, in preparation.
31. J. E. Mentall and H. D. Morgan, *Phys. Rev. A* **14**, 954 (1976).
32. K-H. Tan, F. G. Donaldson, J. W. McConkey, *Can. J. Phys.* **52**, 786 (1974).
33. B. A. Smith *et al.*, *Science* **212**, 163 (1981).
34. T. R. McDonough and N. M. Brice, *Icarus* **20**, 136 (1973).
35. W. A. Smyth, in preparation.
36. D. F. Strobel, *Icarus* **21**, 466 (1974).
37. F. C. Fehsenfeld, A. L. Schmeltekopf, E. E. Ferguson, *J. Chem. Phys.* **46**, 2802 (1967).
38. We thank the Voyager project personnel at JPL for the enthusiastic efforts that have made this mission a success. We thank the staff of the Earth and Space Sciences Institute, Tucson, for their untiring support. This work was supported by the JPL, California Institute of Technology, under NASA contract NAS 7-100. Additional support was provided by the Planetary Sciences Discipline of NASA's Office of Space Sciences.

9 February 1981

Magnetic Field Studies by Voyager 1: Preliminary Results at Saturn

Abstract. *Magnetic field studies by Voyager 1 have confirmed and refined certain general features of the Saturnian magnetosphere and planetary magnetic field established by Pioneer 11 in 1979. The main field of Saturn is well represented by a dipole of moment 0.21 ± 0.005 gauss-*R_S^3 *(where 1 Saturn radius,* R_S*, is 60,330 kilometers), tilted 0.7° ± 0.35° from the rotation axis and located within 0.02* R_S *of the center of the planet. The radius of the magnetopause at the subsolar point was observed to be 23* R_S *on the average, rather than 17* R_S*. Voyager 1 discovered a magnetic tail of Saturn with a diameter of approximately 80* R_S*. This tail extends away from the Sun and is similar to type II comet tails and the terrestrial and Jovian magnetic tails. Data from the very close flyby at Titan (located within the Saturnian magnetosphere) at a local time of 1330, showed an absence of any substantial intrinsic satellite magnetic field. However, the results did indicate a very well developed, induced magnetosphere with a bipolar magnetic tail. The upper limit to any possible internal satellite magnetic moment is* 5×10^{21} *gauss-cubic centimeter, equivalent to a 30-nanotesla equatorial surface field.*

The Voyager 1 magnetic field instrumentation system (*1*) operated normally throughout the Saturn encounter. This report describes preliminary results of data obtained from the multiple range, dual low-field triaxial fluxgate magnetometers mounted on the 13-m boom. For this study, vector measurements at 60-msec intervals were averaged over 1.92, 9.6, and 48 seconds, 16 minutes, and 1 hour. The ranges of the sensors were changed automatically by an onboard system so that the maximum sensitivity of ± 0.0044 nanotesla (nT), while in the lowest range of ± 8.8 nT, decreased to ± 0.513 nT in the ± 2100 nT range near closest approach.

The maximum field measured was 1093 nT, at $\theta = -40.3°$ latitude and $\phi = 184.4°$ longitude, just before closest-approach of 3.07 R_S (1 R_S = 60,330 km). It was somewhat larger than the value of 1010 nT expected on the basis of planetary magnetic field models derived from Pioneer 11 results (*2, 3*). The axis of the magnetic dipole representing the main field of Saturn is almost aligned with the rotation axis (*2, 3*). Thus, Voyager 1 crossed the magnetic equatorial plane only once within 20 R_S, the orbit of Titan, as the spacecraft left the Saturnian magnetosphere at a local time of 0400 and a latitude of 20° to 25°.

One of the most exciting phases of the

0036-8075/81/0410-0211$01.25/0

Saturn encounter was the close flyby at Titan, at a minimum distance of 6969 km from its center. Because of Titan's size, the existence of a substantial atmosphere, and the spacecraft trajectory, this event must be considered as a major planetary encounter in its own right. Two major problem areas were of interest: first, does the plasma, either of solar wind or Saturnian magnetosphere origin, flowing toward Titan interact with an internal magnetic field of Titan (*4*) or with its ionosphere? Second, what are the magnetic field and plasma characteristics of the interaction at Titan, which might occur at different values of the Alfvénic and sonic Mach numbers, as compared with the solar wind interaction at Venus or the Jovian magnetosphere interaction at Io (*5*)?

Bow shock, magnetopause, and magnetosheath. Voyager 1 crossed the bow shock of Saturn only once during its inbound leg toward the planet. The traversal occurred at 2327 SCET (spacecraft event time–Universal Time) on 11 November (day 316) 1980, at a planetocentric distance of 26.1 R_S. Five inbound magnetopause crossings occurred from 0154 to 0248 UT on the next day, that is, shortly after the bow shock crossing (see Table 1 and Fig. 1). The apparent width of the magnetosheath near the subsolar point, relative to the distance from the planet, was less than that observed at Earth or Jupiter. This may be a true spatial feature of the solar wind interaction with Saturn or may be caused by the motion of the bow shock or magnetopause. There were also five outbound magnetopause crossings, the first occurring at 1729 UT on day 319 while the spacecraft was at 43.1 R_S; only one outbound bow shock crossing occurred at about 0618 UT on day 321 at 77.9 R_S (see Table 1).

Table 1. Saturn bow shock (BS) and magnetopause (MP) boundary crossings by Voyager 1.

Type of crossing	Day	Center time (UT)	Distance (R_S)
		Inbound	
BS	316	2327	26.1
MP	317	0154	23.7
MP	317	0214	23.4
MP	317	0229	23.1
MP	317	0242	23.0
MP	317	0247	22.8
		Outbound	
MP	319	1729	43.1
MP	319	1807	43.7
MP	319	2029 ± 12^m	≈ 46.0
MP	319	2100 ± 8^m	≈ 46.5
MP	319	2152	47.2
BS	321	0618 ± 1^m	77.9

The boundary normals of the five inbound magnetopause transitions (durations from 18 to 135 seconds) were determined from the 1.92-second average data by using the minimum variance methods of Siscoe *et al.* (*6*) (method A) and Sonnerup and Cahill (*7*) (method B). The methods gave essentially identical results for the minimum variance direction, assumed to be the magnetopause normal direction; that is, for method A: $\delta_A = -1°$, $\lambda_A = 196°$, and for method B: $\delta_B = 0°$, $\lambda_B = 193°$. This agreement between the two methods is consistent with the magnetopause being a tangential discontinuity, rather than a rotational discontinuity. Method B indicated that, in each case, the magnetopause was a tangential discontinuity within approximately 12°; that is, β ranged between 78° and 89°, where $\beta = \cos^{-1}(\langle B_Z \rangle / B)$ and is 90° for an ideal tangential discontinuity; $\langle B_Z \rangle$ is the average normal component of the field and B is its average magnitude across the discontinuity. Preliminary minimum variance analyses of the outbound magnetopause crossings yielded less conclusive results, because in almost every case the change in field direction across the boundary was too small to yield accurate normal directions.

Figure 2 shows the trajectory of Voyager 1 for 7 days around closest approach (2345 UT of day 317) to the planet; in these coordinates $\hat{X}_0$ and $\hat{Y}_0$ are in the orbital plane of Saturn with $-\hat{Y}_0$ approximately in the direction of planetary motion, $\hat{X}_0$ is sunward, and $\hat{Z}_0$ is "northward." To illustrate the high latitudes that the spacecraft reached after closest approach, the trajectory is shown in cylindrical coordinates, X_0 versus $D = (Y_0^2 + Z_0^2)^{1/2}$. The model magnetopause and bow shock boundaries, as shown in Fig. 2, are based on a parabola and hyperbola, respectively, coincident with *average* crossing positions, inbound and outbound, expressed in cylindrical coordinates, that is, $D(X_0)$ versus X_0, and shown for the X_0-Y_0 plane. The X_0-Y_0 projection of the average magnetopause normals, determined by the minimum variance analyses discussed above, is shown as the vector $\mathbf{N}_{MP}$. This normal direction is consistent with that expected from the model parabolic magnetopause with a subsolar point at about 23 R_S. The crosshatched region extends from the average outbound magnetopause position to the outbound bow shock and therefore represents the average outbound magnetosheath.

Also shown for comparison is the "nearest" inbound and outbound Pioneer 11 magnetosheath regions. We define nearest magnetosheath as that region between the nearest magnetopause and the nearest bow shock, for either inbound or outbound legs of the trajectory. The specific boundaries for Pioneer 11 were taken from Table 1 of Wolfe *et al.* (*8*). If a corresponding "farthest" Pioneer 11 magnetosheath were plotted in Fig. 2, it would lie far outside the figure. Their last bow shock was identified at a radial distance of 102 R_S! The large difference between the Pioneer and Voyager boundary positions is due to

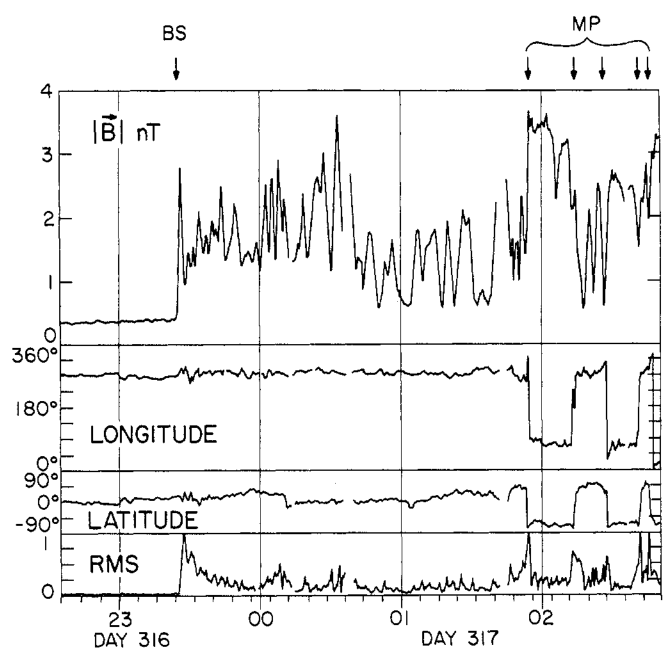

Fig. 1. The observed magnetic field during the interval encompassing the inbound bow shock (*BS*) and magnetopause (*MP*) crossings, in terms of 48-second averages. |B| is the magnitude of the field in nanoteslas (1 nT = 10^{-5} gauss), and the longitude (λ) and latitude (δ) are defined in a spacecraft-centered coordinate frame such that λ is measured azimuthally in a plane parallel to the ecliptic (λ = 90° in the direction of planetary motion since λ = 0° is in the antisolar direction). δ is the inclination angle (= + 90° for a field "northward" of and normal to the ecliptic plane). The RMS, also given in nanoteslas, is the Pythagorean mean root mean square deviation based on the 48-second averaging periods.

differences in the ambient solar wind momentum flux (8, 9).

Encounter overview. Figure 3 presents an overview of the encounter from prior to the inbound bow shock to beyond the outbound bow shock. The field magnitude, Pythagorean root-mean-square (RMS) component deviation, bow shock, and magnetopause crossings are shown. Notice that during the outbound magnetosheath traversal the spacecraft latitude is 24°, whereas near closest approach it is $-40.3°$. The asymmetry in the field magnitude with respect to closest approach is due to a latitude effect and a longitudinal asymmetry of the field as a function of local time.

The increase in the RMS as the spacecraft nears closest approach is due to the spatial gradient of the planetary field and not to temporal changes, as finer time-scale data reveal. However, in the regions bordering the inbound and outbound magnetopause, the enhanced RMS is indeed due to temporal changes, evidently generated by varying external conditions. An example is the increase in the ratio of RMS to the magnetic field, B, for the interval from 1100 to 1807 UT of day 319, where the last 40 minutes or so consists apparently of boundary layer plasma (10) just outside the magnetopause (see Table 1).

The closest approach to Titan (at 0540 UT of day 317) occurred within Saturn's magnetosphere, but observable effects lasted less than 16 minutes and are therefore not readily evident in this overview figure. However, for approximately 2 hours around this region ($R \sim 20\ R_S$), the RMS is moderately enhanced and B is variable, indicating that at the time of closest approach to Titan the background field was not steady (compare this region to that at 20 R_S outbound).

We also noticed differences in the pre- and postencounter interplanetary magnetic fields with respect to RMS level and variations in B. At 10 AU the field is expected, on average, to be nearly aligned with the $\pm\ Y_0$ axis of Fig. 2. Thus, the field will not generally connect the spacecraft to the bow shock from the inbound trajectory but will do so outbound from the planet. It is therefore not surprising that the outbound data, not shown, give evidence of the presence of Saturn in terms of upstream disturbances via this field-line connection to the bow shock.

Magnetosphere and tail. The average magnetic field geometry observed by Voyager 1 in the Saturnian magnetosphere is shown in Fig. 4. Given are the hourly averaged X-Z (Fig. 4a) and X-Y (Fig. 4b) vector component projections along the trajectory. The coordinates are solar magnetospheric (SM), with X toward the sun, Z positive northward and oriented such that the planetary magnetic dipole axis always lies in the X-Z plane. In this analysis it was assumed that there was no angular offset between the magnetic dipole and rotation axes. Therefore, the SM coordinates are a fixed system. Also shown in the figure are curves giving the cylindrically symmetric model magnetopause boundary already described.

The vector data of Fig. 4 clearly illustrate several features of the large-scale Saturnian magnetospheric field. The first is the distinctly southward orientation of the field in the sunward magnetosphere. This is consistent with the Pioneer 11 observations near noon in the outer magnetosphere (3). Also, the field remained approximately in meridian planes throughout the inbound approach to Saturn. Nearer the planet, the average vector field observed by Voyager 1 rapidly changed direction and magnitude as the spacecraft traversed the southern latitude regions of the inner, chiefly dipolar, field in a relatively short time.

On the nightside of the planet, the geometry of the field changed from principally dipolar, lying in meridian planes, to tail-like. The field approached an orientation generally in the antisolar direction and parallel to the model magnetopause until Voyager 1 left the magnetosphere at the relatively high SM latitude of about 23° at a radial distance of 46 R_S

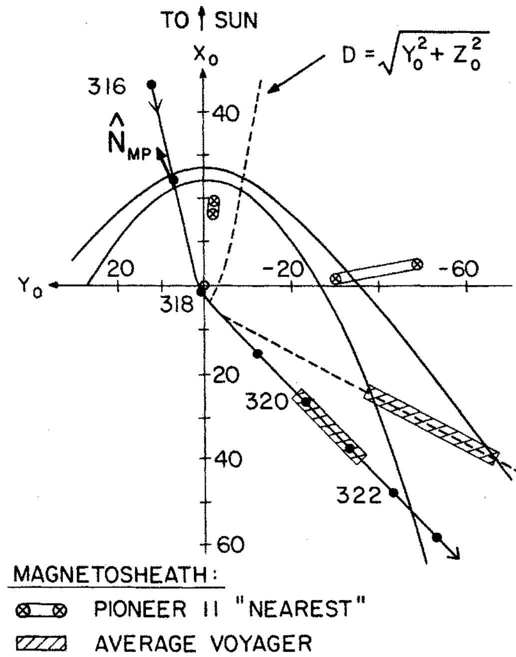

Fig. 2. Voyager 1's trajectory near Saturn in orbital (solid curve) and cylindrical coordinates (dashed curve). Also shown are model bow shock and magnetopause boundaries, projected into the orbital ($X_0 = Y_0$) plane. Distances in Saturn radii (1 R_S = 60330 km).

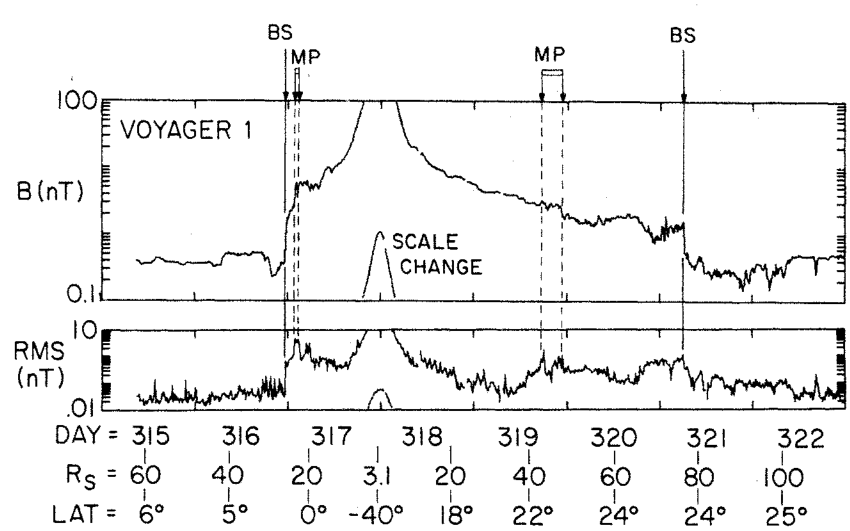

Fig. 3. An overview of the magnitude and Pythagorean mean RMS of the magnetic field for 8 days around closest approach to Saturn. Shown are 16-minute averages. The bottom two scales denote R_S, the planetocentric radial distance of the spacecraft in units of Saturnian radii and latitude (LAT) with respect to Saturn's equator.

($X_{SM} \approx -25\ R_S$). No tail current sheet traversals appear in the Voyager observations, in contrast to the polarity reversals observed at near equatorial latitudes by Pioneer 11 when the spacecraft was outbound near the dawn terminator (*3*). However, some variation in the field can be seen in the data during the traversal of the northern tail lobe. This may represent a temporal change in tail orientation in response to external (solar wind) changes. The field vectors in the tail near the outbound magnetopause in Fig. 4 that have orientations significantly different from the others represent hours in which the magnetopause was observed.

From the outbound field intensity measurements and the position of the outbound magnetopause crossings, it is estimated that the Saturnian magnetic tail diameter is approximately 80 R_S with an average field of ~ 3 nT at $X_{SM} \approx -25$ R_S. To estimate the size of the polar cap region one can assume that the magnetic field in the tail lobes connects directly to the polar caps. Using conservation of flux, we may write

$$B_T = 4\, B_0\, (R_S/R_T)^2 \sin^2 \theta_{pc}$$

where B_T is the average field in the tail lobes, R_T is the tail radius, and θ_{pc} is the colatitude of the polar cap (*11*). Taking $B_T = 2.5 - 3.5$ nT and $R_T = 36\ R_S$ to 40 R_S, one obtains $\theta_{pc} = 11.3°$ to 15.0°, or a latitude range of 78.7° to 75°. This suggests that Saturn has a smaller polar cap auroral zone than that of Earth ($\theta_{pc} = 18°$). Observations of austral polar aurora by the Voyager 1 ultraviolet spectrometer experiment yields a location that is in agreement with this smaller auroral zone (*12*).

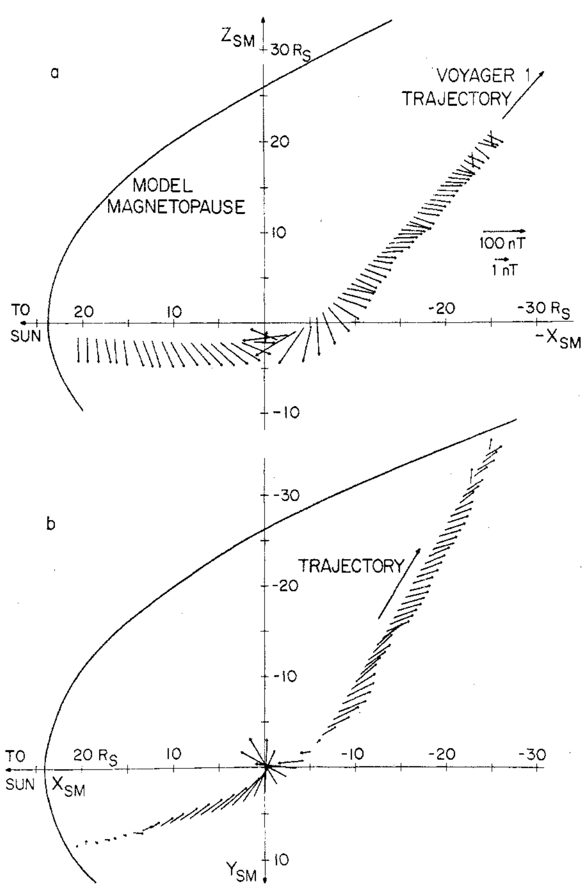

Fig. 4. Projection of hourly average magnetic field components in the Saturnian magnetosphere onto the solar magnetospheric (*SM*) *X-Z* (a) and *X-Y* (b) planes along the Voyager 1 trajectory. A logarithmic scale has been used to represent field magnitude as indicated.

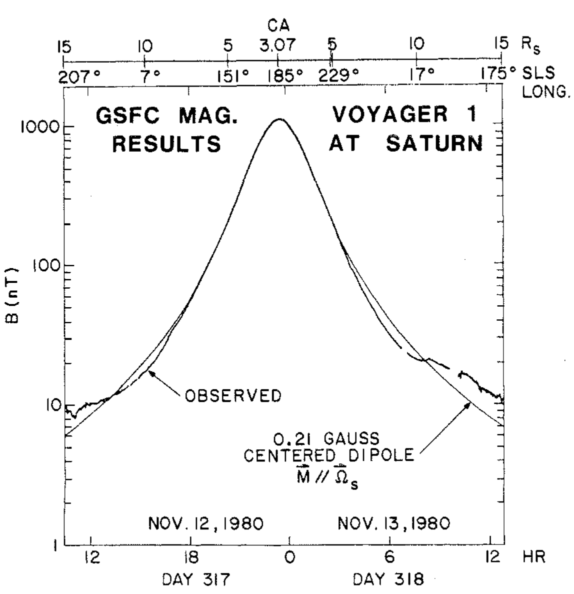

Fig. 5. Observed magnitude of magnetic field close to Saturn ($R < 15\ R_S$) and comparison with the internal field model described in text. Averages over 48 seconds are used in this presentation. Note the increasing departure from a dipole evident for $R > 8\ R_S$.

Inner magnetosphere and intrinsic planetary field. In contrast to the Pioneer 11 encounter trajectory where the spacecraft remained within 6° of the equatorial plane, the Voyager 1 trajectory provided a unique opportunity to sample relatively high latitudes (−40°) at close radial distances (3.07 R_S). The maximum measured field near closest approach to the planet was 1093 nT, somewhat larger than anticipated based on the magnetic field models derived from the Pioneer 11 observations (*2*, *3*).

In the inner region, $R < 10\ R_S$, the observations do not show any large and significant temporal variations. The observed field can be attributed to sources residing in the interior of the planet plus a relatively small contribution from an external current system.

The traditional method of representing planetary magnetic fields by means of orthogonal spherical harmonic expansions assumes that the field is derivable from a scalar potential, implying that no currents flow in the region where the measurements are obtained. This condition is rather well satisfied within the radial range $R < 6\ R_S$. The analyses reported here utilize 48-second averaged field values and preliminary spacecraft attitude data, and may be revised subject to improvements in engineering information. The planet-centered longitude of the spacecraft was derived from the radio-determined Saturn longitude system (SLS) proposed by Desch and Kaiser (*13*) using a planet rotation period of 10 hours 39.4 minutes.

Using data within 6 R_S, we find a primarily dipolar internal field, with the dipole axis nearly parallel with the planet's rotation axis, as suggested by Pioneer 11 studies (*2*, *3*). The dipole axis tilt, however, is definitely nonzero, ~ 0.7°, tilted toward an SLS longitude of 331°. The best fitting (RMS = 2.7 nT) spherical harmonic model, assuming 1 internal order and 1 external order (I1E1), has the following Schmidt normalized coefficients: g_1^0 = 0.209 gauss, g_1^1 = 0.00220 gauss, and h_1^1 = 0.00124 gauss; external G_1^0 = − 8.8 nT, G_1^1 = − 4.2 nT, and H_1^1 = 3.3 nT. Second-order (quadrupole) models do not provide a significant reduction in the residuals compared to dipolar models incorporating an external field. Derived quadrupole terms are small and may not be adequately resolved with Voyager 1 observations alone. We estimate the dipole displacement to be less than ~ 0.02 R_S. Although Pioneer 11 went much closer to Saturn (1.35 R_S), the axial offset inferred [$\Delta \approx$ 0.04 to 0.05 R_S (2, 3)] is derived from the most poorly determined quadrupole term (g_2^0). This can be understood by recalling that Pioneer 11 made a near equatorial pass through the Saturnian magnetosphere.

Figure 5 displays the magnitude of the observed field compared with that of a centered dipole with a moment of 0.21 gauss-R_S^3, for radial distances less than 15 R_S. The dipolar nature of the field is clearly illustrated by the excellent fit to the simple model. These data also show clear evidence of a large-scale, azimuthal current system extending radially throughout much of Saturn's equatorial magnetosphere. The observed field magnitude at radial distances of less than 10 R_S is significantly reduced by the largely solenoidal field of the (eastward) azimuthal currents; the discontinuity in slope of the observed field magnitude at about hour 17 on day 317 occurs as Voyager 1 emerges from the current-carrying region while inbound to periapsis. Analyses suggest a magnetodisk current sheet similar to Jupiter's (*14*) extending from about 8 to about 16 R_S in the equatorial plane and with a total thickness of approximately 4 R_S. Current densities are an order of magnitude less than those observed at Jupiter.

Thus Saturn is similar to Earth in terms of its average surface magnetic field strength. Its magnetosphere is similar to Jupiter's in that each possesses a large-scale azimuthal current system confined to an equatorial annular disk. But Saturn appears to be unique with respect to the near alignment of magnetic and rotational axes. The small tilt of the dipole axis (~ 0.7°) is the only longitudinal asymmetry that we have identified. A comparison of Pioneer 11 and these Voyager 1 results for the dipole term describing the main field of Saturn is shown in Fig. 6. The small tilt of the dipole of Saturn now appears certain but is, at present, not a plausible source of the magnetic anomaly in the northern hemisphere responsible for the modulation of radio emission (*13*).

Encounter with Titan. As noted by Acuña *et al.* (*2*), Titan's orbital distance of 20 R_S is equal to that of the average magnetopause stagnation point distance, so that Titan can be immersed in the magnetosheath or even the interplanetary medium when near local noon. The Titan encounter occurred during the inbound passage of Saturn's magnetosphere at a local time of 1330 (see Fig. 2). From the discussion of the multiple magnetopause crossings and the general variability of the magnetic field, it follows that appreciable dynamical variations occurred in the outer magnetosphere. Therefore, no simple assumption can be made concerning the direction and magnitude of the plasma velocity and magnetic field vectors of the flow incident on Titan. Even the assumption of constancy of the incident flow during the half hour centered on closest approach cannot be justified a priori.

The trajectory of Voyager 1 relative to Titan is shown in Fig. 7, a and b. Closest approach occurred at 0540:20 UT and the orbital plane of Titan was crossed at 0543:07 UT from north to south. The inclination of the trajectory with respect to the orbital plane of Titan was 8.7°, while the flyby speed of Voyager 1 relative to Titan was 17.3 km/sec. The trajectory was therefore an almost ideal diametrical passage through Titan's geometrical wake, in the sense of corotational flow of the Saturnian magneto-

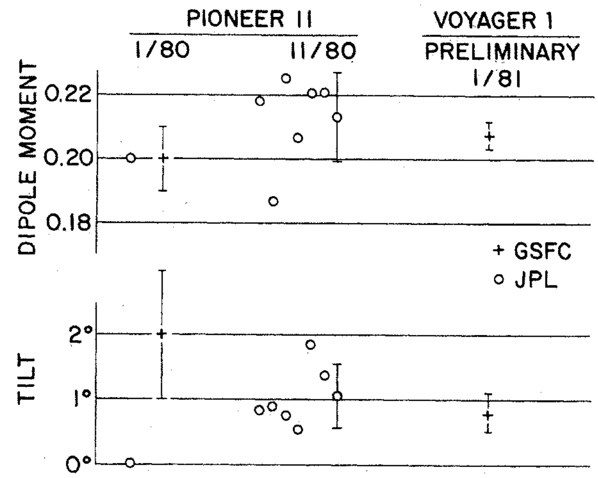

Fig. 6. Comparison of dipole moment and tilt angle (relative to rotation axis) of models of the Saturnian main dipole field determined by Pioneer 11 (*3*) and Voyager 1 (*2*). The uncertainties for these preliminary Voyager 1 results represent a best estimate of the errors associated with spacecraft attitude, position, measurements, and physical validity of the field models. The JPL Pioneer 11 values represent different models whose average and standard deviation are shown (*3*).

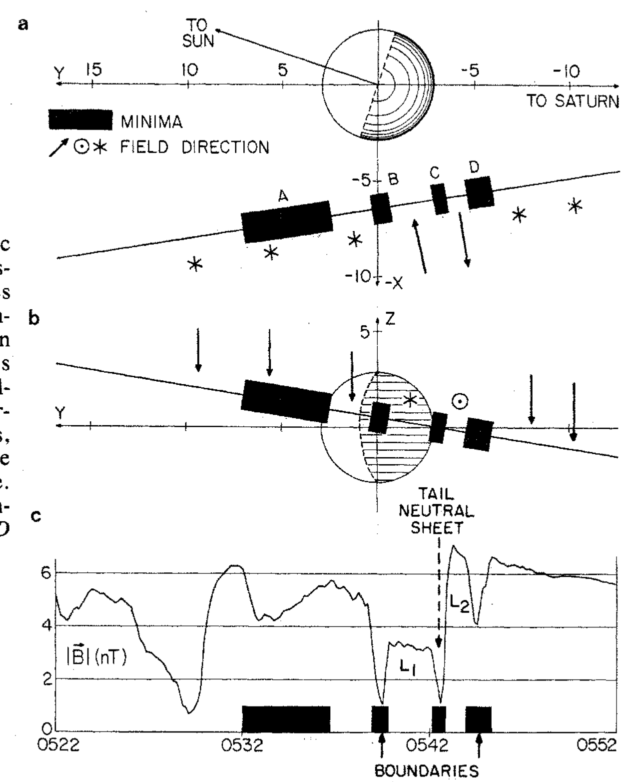

Fig. 7. Magnitude of magnetic field observed near Titan closest approach using averages over 9.6 seconds. Upper panels display the trajectory in Titan-centered coordinates with the *Y* axis directed radially outward from Saturn, *Z* parallel to Saturn's rotation axis, and *X* "upstream" from the corotating magnetosphere. See text for discussion of interpretation of events *A* to *D* and features L_1 and L_2.

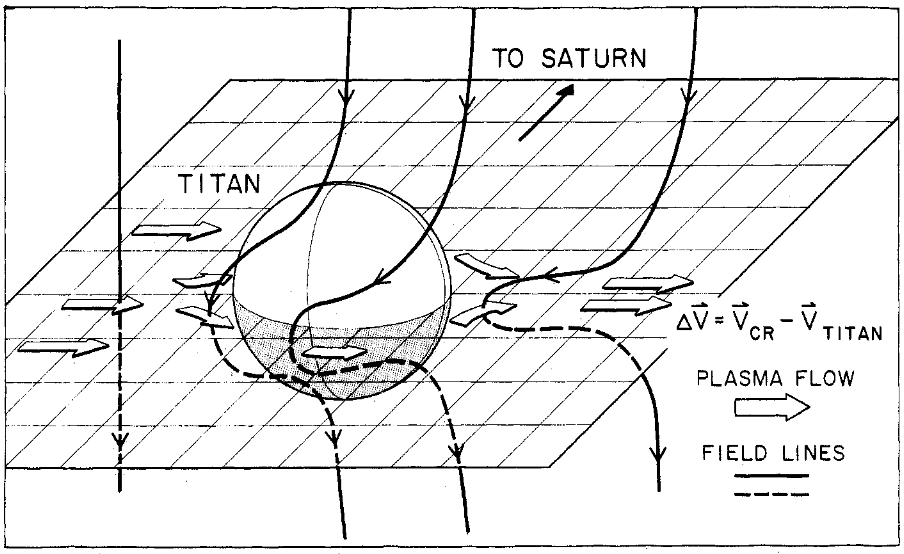

Fig. 8. Sketch of distorted Saturn magnetospheric field in vicinity of Titan, caused by induced currents in the ionosphere and tail wake of Titan. Bipolar magnetic tail field formation is seen to be due to "draping" of field lines around Titan's ionosphere, forming the tail, which leads Titan in its orbit around Saturn.

sphere. The magnitude of the magnetic field as a function of time during the encounter is shown in Fig. 7c. Also shown is a sketch of the magnetic field directions along two projections of the spacecraft trajectory relative to Titan.

It is obvious from the magnitude plot that an appreciable internal magnetic moment is excluded by the data. As a conservative estimate, a dipolar field of 30 nT on Titan's equator [1 Titan radius (R_T) = 2570 km] would have been observable near closest approach. A more refined analysis in the future is expected to lead to more accurate limits on an internal field. Direct application of Busse's law would lead to a core size of less than 700 km for a dynamo-active metallic convecting region (4).

Since Titan has no appreciable intrinsic magnetic field and associated magnetosphere, there is a direct interaction between the Saturnian magnetoplasma and the ionosphere-atmosphere system of Titan. No obvious fast shock signature can be identified in our data. This implies that the magnetohydrodynamic fast Mach number cannot be much greater than one, that is, $V_S < (V_A^2 + a^2)^{1/2}$. Here we have used the Saturnian corotation plasma velocity V_S, ~ 200 km/sec, the local Alfvén speed V_A, and the sonic speed a, respectively, as well as the assumption that the flow does not deviate too much from perpendicular flow (the consistency of the latter assumption will be shown later). Hence, at least one of the Mach numbers M_A or M_S must be less than one, from the absence of a fast shock alone.

Recently, Jones *et al.* (15) discussed Pioneer 11 magnetic field observations near Saturn's dawn meridian, which were made at about 145 Titan radii (R_T) approximately along the corotation direction. They suggested that a supersonic interaction of Saturn's magnetosphere with Titan was observed, which produced a relatively strong magnetoacoustic shock with an asymptotic shock cone angle of 20.5°. Since the Voyager 1 data show no evidence for such a shock, as observed by Pioneer 11, either conditions were different when and where Voyager 1 passed Titan or the Pioneer 11 signature may be unrelated to Titan. They noted that the signature may have resulted from near penetration of several possible current systems detected in Saturn's magnetosphere.

Physically, an atmosphere-plasma interaction leads to an induced magnetosphere with a draping of field lines around the ionopause, as sketched in Fig. 8. The directions in Fig. 7 are consistent with this draping. On its passage through the wake region from north to south, the spacecraft first observes field lines directed toward Titan and after the deep minimum in magnitude C at 0542:30, the field lines point away from Titan. This dip C corresponds to the current sheet separating the northern and southern lobes of the induced bipolar magnetic tail. In agreement with this interpretation, the tail neutral sheet occurs very close to the crossing of the orbital plane of Titan, as expected for a corotational flow, and an upstream field of "vertical" orientation. The induced voltage across this "unipolar inductor," developed as the Saturnian magnetospheric plasma sweeps past Titan, is approximately 6000 V. This drives an induced current system whose magnetic field distorts the background field and leads to the magnetic field configuration that we qualitatively describe as draped field lines.

Having identified draping and the presence of a tail neutral sheet, the other features in Fig. 7 have been interpreted as follows. The dips B at 0539:30 and D at 0544:30 UT are the inbound and outbound crossings of the boundaries of Titan's induced magnetic tail. The tail width is determined by the transverse width of the field draping region and finite gyroradius effects. The broad feature A, from 0532 to 0537 UT, may be a consequence of the dayside hydrogen corona (12), possibly combined with some temporal variations in the Saturnian magnetosphere. The dip around 0529 is probably not due to the deflected flow pattern observed around closest approach. It may be a remanent of the wake of Titan one or more Saturn rotations previously (9).

Returning to the induced tail, we note two interesting features in Fig. 7. The tail is deflected from the corotation direction and it is asymmetric. The simplest explanation for the deflection is a deviation of plasma flow from corotation. Also, we expect contributions due to the longitudinal asymmetry of the atmosphere-ionosphere of Titan, finite gyroradius effects, or the Hall effect. Even a weak internal magnetic field may marginally influence the plasma flow. The asymmetry may be explained by an atmospheric east-west or north-south asymmetry, the influence of a weak internal field, the plasma effects mentioned above, or a combination of these factors. For example, the atmospheric asymmetry provided by the sun's radiation would lead to stronger plasma-loading of the field lines observed before the crossing of the tail neutral sheet. The associated pressure of the plasma will force the plasma to expand to adjust approximately to the surrounding total pressure. This expansion may explain the reduced field in the first observed lobe (L_1). It would be expected to be absent in the second lobe (L_2), as observed. The total inward and outward magnetic flux in the induced magnetic tail lobes are approximately equal, as expected for an induced tail field. If one assumes an extension of about one R_T perpendicular to the orbital plane, flux conservation leads to a semiannular pile-up region of about 600 km thickness ahead of Titan. This estimate will be modified when the asymmetry is taken into account.

We conclude that the Saturnian magnetoplasma interacted with the ionosphere-atmosphere system of Titan, leading to the formation of an induced magnetosphere and bipolar magnetic tail. This induced magnetosphere was observed to be deflected from the corotational flow direction and was also asymmetric with respect to the tail neutral sheet. Possible explanations include asymmetries of the atmosphere, finite gyroradius effects for the deflection, and a deviation from corotational flow. The upper limit for the magnetic moment of a possible internal magnetic field is 5×10^{21} gauss-cm^3, consistent with at most a small convective, metallic core. This is, again, in agreement with the mean density and composition arguments.

NORMAN F. NESS
MARIO H. ACUÑA
RONALD P. LEPPING
JOHN E. P. CONNERNEY
KENNETH W. BEHANNON
LEONARD F. BURLAGA
Laboratory for Extraterrestrial Physics, Goddard Space Flight Center Greenbelt, Maryland 20771
FRITZ M. NEUBAUER
Technische Universität, Braunschweig, Federal Republic of Germany

References and Notes

1. K. W. Behannon, M. H. Acuña, L. F. Burlaga, R. P. Lepping, N. F. Ness, F. M. Neubauer, *Space Sci. Rev.* **21**, 235 (1977).
2. M. H. Acuña, J. E. P. Connerney, N. F. Ness, *J. Geophys. Res.* **85**, 5675 (1980).
3. E. J. Smith, L. Davis, Jr., D. E. Jones, P. J. Coleman, Jr., D. S. Colburn, P. Dyal, C. P. Sonett, *ibid.*, p. 5655.
4. F. M. Neubauer, *Geophys. Res. Lett.* **5**, 905 (1978).
5. M. H. Acuña, F. M. Neubauer, N. F. Ness, *J. Geophys. Res.*, in press; F. M. Neubauer, *ibid.* **85**, 1171 (1980).
6. G. L. Siscoe, L. Davis, Jr., P. J. Coleman, Jr., E. J. Smith, D. E. Jones, *J. Geophys. Res.* **73**, 61 (1968).
7. B. U. O. Sonnerup and L. J. Cahill, Jr., *J. Geophys. Res.* **72**, 171 (1967).
8. J. H. Wolfe, J. D. Mihalov, H. R. Collard, D. D. McKibbin, L. A. Frank, D. S. Intriligator, *Science* **207**, 403 (1980).
9. H. S. Bridge *et al.*, *Science* **212**, 217 (1981).
10. J. Scudder, private communication.
11. N. F. Ness, *J. Geophys. Res.* **70**, 2989 (1965).
12. A. L. Broadfoot *et al.*, *Science* **212**, 206 (1981).
13. M. L. Kaiser, M. D. Desch, J. B. Warwick, J. B. Pearce, *Science* **209**, 1238 (1980); M. D. Desch and M. L. Kaiser, *Geophys. Res. Lett.* **8**, in press.
14. J. E. P. Connerney, M. H. Acuña, N. F. Ness, *J. Geophys. Res.* **86**, in press.
15. D. E. Jones, B. T. Tsurutani, E. J. Smith, R. J. Walker, C. P. Sonett, *J. Geophys. Res.* **85**, 5835 (1980).
16. We thank our colleagues in the Voyager Project, especially the Plasma Science Team (H. S. Bridge, principal investigator) for discussions of these early results, and the entire Voyager team at JPL for the success of this experiment. We also thank G. Sisk, E. Franzgrote, and M. DeGyurky of JPL for their support; C. Moyer, J. Scheifele, J. Seek, and E. Worley for contributions to the design, development, and testing at GSFC of the experiment instrumentation; and the data processing staff of the Laboratory of Experimental Physics at GSFC under the direction of W. Mish for their outstanding and dedicated support. One of us, F.M.N., was supported financially by the German Ministry of Science and Technology.

9 February 1981

Plasma Observations Near Saturn: Initial Results from Voyager 1

Abstract. *Extensive measurements of low-energy plasma electrons and positive ions were made during the Voyager 1 encounter with Saturn and its satellites. The magnetospheric plasma contains light and heavy ions, probably hydrogen and nitrogen or oxygen; at radial distances between 15 and 7 Saturn radii* (R_S) *on the inbound trajectory, the plasma appears to corotate with a velocity within 20 percent of that expected for rigid corotation. The general morphology of Saturn's magnetosphere is well represented by a plasma sheet that extends from at least 5 to 17* R_S, *is symmetrical with respect to Saturn's equatorial plane and rotation axis, and appears to be well ordered by the magnetic shell parameter* L *(which represents the equatorial distance of a magnetic field line measured in units of* R_S). *Within this general configuration, two distinct structures can be identified: a central plasma sheet observed from* L = 5 *to* L = 8 *in which the density decreases rapidly away from the equatorial plane, and a more extended structure from* L = 7 *to beyond 18* R_S *in which the density profile is nearly flat for a distance* $\pm$ *1.8* R_S *off the plane and falls rapidly thereafter. The encounter with Titan took place inside the magnetosphere. The data show a clear signature characteristic of the interaction between a subsonic corotating magnetospheric plasma and the atmospheric or ionospheric exosphere of Titan. Titan appears to be a significant source of ions for the outer magnetosphere. The locations of bow shock crossings observed inbound and outbound indicate that the shape of the Saturnian magnetosphere is similar to that of Earth and that the position of the stagnation point scales approximately as the inverse one-sixth power of the ram pressure.*

This is a preliminary report of the observations made by the plasma science experiment on Voyager 1 during the Saturn encounter period. The relevant instrument characteristics are discussed briefly in a report of the Jupiter encounter (*1*); a detailed description is available in (*2*). We discuss here (i) the bow shock and magnetopause crossings; (ii) the spatial distribution, composition, and flow of the magnetospheric plasma; (iii) the configuration of the plasma sheet; (iv) the interaction between Titan and the magnetospheric plasma; and (v) Titan and the atomic hydrogen torus as sources of plasma.

Boundary crossings. As Voyager 1 approached Saturn, a single bow shock crossing was observed on 11 November 1980 at 2326 [all times in this report are spacecraft event times in universal time; and distances given in units of Saturn radii (R_S) refer to an equatorial radius of 60,330 km]. Five magnetopause crossings occurred between 0154 and 0248 on 12 November. The spacecraft remained inside the magnetosphere until 14 November, when it again crossed the magnetopause boundary five times and then reentered the interplanetary wind on 16 November (Table 1). The times of bow shock crossings (both inbound and outbound) compare well with those expected on the basis of a bow shock shape observed for Earth (*3*), the solar wind ram pressure (P), the position of the first

Table 1. Bow shock and magnetopause crossings and external wind parameters.

Boundary	Time*		Distance (R_S)
	Inbound crossings		
Shock	11 November	2326	26.1
Magnetopause	12 November	0154	23.6
		0213	23.4
		0228	23.2
		0242	22.9
		0248	22.7
	Outbound crossings		
Magnetopause	14 November	1729	42.7
		1806	43.4
		2034	45.7
		2115	46.1
		2140	46.9
Shock	16 November	0619	77.4
	External solar wind parameters		
11 November: 420 km/sec, 0.11 cm^{-3}, flow from sun			
16 November: 460 km/sec, 0.16 cm^{-3}, flow from 4° above ecliptic			

*Times are approximate entries into and exits from the magnetosheath and do not reflect the boundary layer phenomena which are observed.

0036-8075/81/0410-0217$02.00/0